Extracting jet transport coefficient from jet quenching at RHIC and LHC

Chang Ning Bo,[1,2] Karen M. Burke,[3] Alessandro Buzzatti,[4,5] Charles Gale,[6] Miklos Gyulassy,[5] Ulrich Heinz,[7] Sangyong Jeon,[6] Abhijit Majumder,[3] Guanyou Qin,[2,3] Björn Schenke,[8] Chun Shen,[7] Xin-Nian Wang,[2,4] Jiechen Xu,[5] Clint Young,[6] and Hanzhong Zhang[2]

[1] *School of Physics, Shandong University, Jinan, Shandong 250100, China*
[2] *Institute of Particle Physics and Key Laboratory of Quarks and Lepton Physics (MOE), Central China Normal University, Wuhan 430079, China*
[3] *Department of Physics and Astronomy, Wayne State University, Detroit, Michigan 48201, USA*
[4] *Nuclear Science Division, MS 70R0319, Lawrence Berkeley National Laboratory, Berkeley, California 94720, USA*
[5] *Department of Physics, Columbia University, New York 10027, USA*
[6] *Department of Physics, McGill University, 3600 University Street, Montreal, Quebec, H3A 2T8, Canada*
[7] *Department of Physics, The Ohio State University, Ohio 43210, USA*
[8] *Department of Physics, Brookhaven National Laboratory, Upton, New York 11973, USA*

Within four different approaches to parton propagation and energy loss in dense matter, a phenomenological study of experimental data on suppression of large p_T single inclusive hadrons in heavy-ion collisions at both RHIC and LHC was carried out. The evolution of bulk medium used in the study for parton propagation was given by 2+1D or 3+1D hydrodynamic models which are also constrained by experimental data on bulk hadron spectra. Values of jet transport parameter $\hat{q}$ at the center of the most central heavy-ion collisions are extracted or calculated within each model whose parameters about the medium properties are constrained by the experimental data on hadron suppression factor R_{AA}. We find that $\hat{q} \approx 0.65$ – 1.1 GeV^2/fm in Au+Au collisions at $\sqrt{s} = 200$ GeV/n and $\hat{q} \approx 1.14$ –1.96 GeV^2/fm in Pb+Pb collisions at $\sqrt{s} = 2.76$ TeV/n for a quark with initial energy of 10 GeV at an initial time $\tau_0 = 0.6$ fm/c. Comparing to earlier studies, these represent significant convergency on values of extracted jet transport parameter due to recent advances in theory and availability of new experiment data from LHC.

I. INTRODUCTION

In the search and study of the quark-gluon plasma (QGP) in high-energy heavy-ion collisions, jet quenching processes play an essential role as hard probes of the properties of dense matter. Because of the hard scales involved, jets are produced in the very early stage of the collisions and their initial production rate can be calculated within perturbative QCD. During their subsequent propagation through the dense medium, interaction between jets and medium will lead to jet energy loss and suppression of final jets and large transverse momentum hadron spectra. Original theoretical studies based on this principle [1]–[17] and collaborative work by the Hard Probes Collaboration on the survey of hard processes in the absence of a hot or dense QCD medium [18, 19] formed the basis for the initial success of the RHIC experimental program on hard probes and the phenomenological studies that ensued.

Since the start of the Relativistic Heavy-ion Collider (RHIC) experimental program, we see not only the suppression of single inclusive hadron spectra at large transverse momentum [20, 21] but also back-to-back high p_T dihadron [22] and γ-hadron correlations [23–25]. The same jet quenching patterns are also observed in the latest heavy-ion collisions at the Large Hadron Collider (LHC) [26–28]. In addition, one has also observed the predicted suppression of reconstructed jets [29–31], as well as increased dijet [32, 33] and γ-jet asymmetry [34, 35]. These observed jet quenching phenomena in heavy-ion collisions at RHIC have been studied within many models [36–48] that incorporate parton energy loss as jets propagate through dense matter. Though many models can describe the observed jet quenching at RHIC quite well, new data from LHC experiments have verified some of the model predictions [49–51] while prove to be a challenge for others [26, 27, 52]. Even within those models that can describe experimental data, the combined data from experiments at RHIC and LHC provide unprecedented constraints on the parameters of medium properties as probed by jet quenching.

One of the programmatic goals of heavy-ion collisions is to extract important medium properties from phenomenological studies of combined experimental data on a wide variety of jet quenching measurements. This is also one of goals of the JET Collaboration. As a first step toward such a goal in this paper, we carry out a survey study of medium properties within some of the existing approaches to parton energy loss in medium as constrained by experimental data on suppression of large transverse momentum single inclusive hadron spectra at RHIC and LHC. We will work within four difference approaches to parton energy loss: GLV-CUJET, HT-M, HT-BW and MARTINI-AMY. GLV uses a potential model for multiple scattering in the medium in which the controlling parameters for energy loss are the strong coupling constant and Debye screening mass. Within high-twist approaches, jet transport coefficient or averaged transverse momentum broadening squared per unit length is the only medium property that affect the parton energy loss. MARTINI-AMY model is based on HTL resummed thermal field theory in which the only adjustable parameter is the strong coupling constant. To have a common ground for this survey study, we focus on jet transport coefficient as given by each of the parton energy loss models. We fit experimental data on jet quenching and then use the parameters that are constrained by the data to calculate jet transport coefficient within that model (GLV-CUJET and MARTINI-AMY).

Since the energy loss or medium modification of the final hadron spectra depends on the space-time profile of parton density in the medium, any systematic and qualitative extraction of the properties of the medium through phenomenological study of jet quenching has to take into account the dynamical evolution of the bulk matter [53–55]. For our current study, 3+1D or 2+1D ideal or viscous hydrodynamic simulations provide the most realistic and dynamic evolution of the bulk medium available that are constrained by experimental data on bulk hadron production, including charged hadron spectra and their azimuthal anisotropies. Uncertainties in jet quenching calculations as a result of variations in hydrodynamic bulk evolution due to different hydro initial conditions and values of viscosity should be small once they are constrained by the experimental data on bulk hadron productions in heavy-ion collisions.

Similar efforts to extract values of the jet quenching parameter have been made before [53, 54] but with diverging values from different models varying as much as a factor of 8. This work will take advantage of the significant progress in our theoretical understanding and modeling of jet quenching and of the evolving medium created in heavy-ion collisions at RHIC and LHC and evaluate the range of jet transport parameters allowed by the combined experimental data at RHIC and LHC. Furthermore, availability of new data on heavy-ion collisions at LHC where higher initial temperature is reached and the range of p_T is much larger than at RHIC, we can for the first time investigate the temperature and jet energy dependence of the jet transport coefficient.

II. GLV-CUJET MODEL

The GLV model [56] correctly predicted in 2002 the general form of the $\sqrt{s}$ evolution of the high p_T pion nuclear modification factor $R_{AA}(p_T, \eta = 0; \sqrt{s}, b) = dN_{AA\to\pi}/(T_{AA}(b)dN_{pp\to\pi}$ from SPS,RHIC to LHC energies. GLV was generalized to include thermal mass and heavy quark effect in DGLV[57]. However in 2005 PHENIX discovered DGLV significantly under-predicted quenching of charm and bottom quark jets. This led to the WHDG[58] generalization of DGLV[57] theory to check whether quenching effects due to elastic energy loss and more realistic jet path length fluctuations could account for the non-photonic electron spectrum from heavy quark meson decay data from PHENIX at RHIC. We found that those effects did not solve the "heavy quark jet puzzle". This led to the dynamical generalization of DGLV[59] replacing the GW static color electric scattering center into the Hard Thermal Loop (HTL) weakly coupled Quark Gluon Plasma ansatz. The jet medium interactions with a HTL QGP medium include dynamic color magnetic as well as static color electric interactions.

The CUJET1.0 Monte Carlo code was developed at Columbia University as part of the Topical JET Collaboration project. With this code we were able to predict the full jet quenching pattern for both light (π) and heavy flavor (D and B) hadrons at both RHIC and LHC including dynamical DGLV, elastic energy loss, as well as full space+time evolution background of the HTL QGP bulk medium. The CUJET1.0 code features: (1) a dynamical jet interaction potentials that can interpolate between pure HTL dynamically screened magnetic and static electric screening limits; (2) the ability to calculate high order opacity corrections up to 9th order in opacity; (3) integration over jet path in diffuse nuclear geometries including Bjorken longitudinally expanding HTL QGP; (4) inclusion of local multi-scale running coupling effects and explore nonperturbative deformations of HTL screening scales; (5) elastic energy loss with fluctuations; (6) evaluate the convolution over numerical initial jet spectra from pQCD parton model; and (7) convolute over jet fragmentation functions and semileptonic final decay into non-photonic electrons.

CUJET1.0 succeeded in explaining for the first time [60] the anomalous high quenching of non-photonic electrons within a pure HTL QCD paradigm and thus a natural solution to the heavy quark jet puzzle due to enhanced dynamical magnetic scattering effects. It further predicted a novel inversion of the $\pi < D < B$ flavor ordering of R_{AA} at high p_T that is yet to be tested at RHIC and LHC.

One of the surprising [61] LHC discoveries was the similarity between R_{AA} at RHIC and LHC despite the doubling of the initial QGP density from RHIC to LHC. CUJET1.0 was able to quantitatively explain this by taking into account the multi-scale running of the QCD coupling $\alpha(Q^2)$ in the DGLV opacity series. At first order in opacity the running coupling rcDGLV induced gluon radiative distribution is given by [62]

$$x\frac{dN_{Q->Q+g}}{dx}(\mathbf{x},\phi) = \int d\tau \rho_{QGP}(\mathbf{x}+\hat{\mathbf{n}}(\phi)\tau,\tau)\int\frac{d^2\mathbf{q}}{\pi}\frac{\alpha_s(\mathbf{q}^2)}{(\mathbf{q}^2+f_E^2\mu^2(\tau))(\mathbf{q}^2+f_M^2\mu^2(\tau)}\int\frac{d^2\mathbf{k}}{\pi}\alpha_s(k_T^2/(x(1-x))$$
$$\times\frac{12(\mathbf{k}+\mathbf{q})}{(\mathbf{k}+\mathbf{q})^2+\chi(\tau)}\cdot\left(\frac{(\mathbf{k}+\mathbf{q})}{(\mathbf{k}+\mathbf{q})^2+\chi(\tau)}-\frac{\mathbf{k}}{\mathbf{k}^2+\chi(\tau)}\right)\left(1-\cos\left[\frac{(\mathbf{k}+\mathbf{q})^2+\chi(\tau)}{2x_+E}\,\tau\right]\right)\,.$$

where $\mu^2(\tau) = 4\pi\alpha_s(4T^2)$ is the local HTL color electric Debye screening mass squared in a pure gluonic plasma with local temperature $T(\tau) \propto \rho_{QGP}^{1/3}(\mathbf{x},\tau)$ along the jet path $\mathbf{x}(\tau)$ through the plasma. Here $\chi(\tau) = M^2x_+^2 + f_E^2\mu^2(T(\tau))(1-x_+)/\sqrt{2}$ controls the "dead cone" and LPM destructive interference effects due to both the finite quark current mass M, and a thermal gluon $m_g = f_E\,\mu(T)/\sqrt{2}$ mass.

We use the HTL deformation parameters (f_E, f_M) to vary the electric and magnetic screening scales relative to HTL. In general HTL deformations could also change $m_g(T)$. The default HTL plasma is $(1,0)$ but we also consider a deformed $(2,2)$ plasma model motivated by lattice QCD screening data. We used the vacuum running $\alpha_s(Q^2) = \min[\alpha_{max}, 2\pi/9\log(Q^2/\Lambda^2)]$ characterized by a nonperturbative maximum value α_{max}. The parameters (α_{max}, f_E, f_M) are therefore our main model control parameters.

The computational task performed via Monte Carlo integration is to evaluate dN_g/dx for each $(\mathbf{x},\hat{n})$ initial jet production coordinates, convolute the inclusive gluon spectrum via a Poisson ansatz to estimate effects of multi-gluon fluctuation, evaluate the normalized radiation probability, $P_{rad}(\Delta E_{rad}, E_0; \mathbf{x}, \hat{n}))$ via fast Fourier transform including delta function $\Delta E/E_0 = 0, 1$ end point sigularities. Multiple running coupling elastic energy loss probability, $P_{el}(\Delta E_{el}, E_0; \mathbf{x}, \hat{n}))$ is computed, and then convoluted $P_{rad} \otimes P_{el}$ with probability for radiative energy loss. The final total energy loss probability is then folded over the initial parton jet spectrum $dN_{pp}/d^2p_T d\eta$. Finally CUJET averages over initial jet configurations via $\int d^2\mathbf{x} d^2\hat{n} T_A(\mathbf{x}+\mathbf{b}/2)T_A(\mathbf{x}-\mathbf{b}/2)$ and fragments jets into different flavor hadrons or leptons to compare with data.

Recently, CUJET1.0 is coupled to more realistic 2+1 D viscous hydro fields [64, 65] tabulated by the hydro group within the JET Collaboration. The hydro temperature fields used in CUJET2.0 are thus constrained by fits to experimental data on bulk low $p_T < 2$ GeV/c spectra. The effects of azimuthally asymmetric radial flow can then be computed in the current CUJET2.0=rcDGLV+VISH C++ code.

Our first results indicate the existence of multiple solutions in the 3D (α_{max}, f_E, f_M) model parameter space compatible with measured RHIC and LHC data on central $R^{\pi}_{AA}(p_T; \sqrt{s}, b)$. The pure HTL solution is $(0.25, 1, 0)$ but we also found a nonperturbative solution $(0.4, 2, 2)$ that is compatible with lattice QCD screening and jet medium coupling. The results are as yet preliminary and under more detailed scrutiny. Our goal is to map out the shape of model space constrained by the data.

The physics implications of these solutions can be visualized by computing the effective jet transport coefficient $\hat{q}(E, T; \alpha_{max}, f_E, f_M) = \int dq^2 q^2 d\sigma/dq^2\rho$ in an idealized static and homogeneous thermal equilibrium medium. This jet transport coefficient $\hat{q}$ depends on jet energy E and local temperature T variation which can be also influenced by values of α_{max} as well as possible electric and magnetic screening mass deformations (f_E, f_M). It is important to emphasize that the $\hat{q}$ varies continuously with the model control parameters (α_{max}, f_E, f_M).

III. HIGHER-TWIST-BERKELEY-WUHAN (HT-BW) MODEL

Within a high-twist approach (HT) [12, 13], the medium-modified quark fragmentation functions are given by

$$\tilde{D}_q^h(z_h, Q^2) = D_q^h(z_h, Q^2) + \frac{\alpha_s(Q^2)}{2\pi}\int_0^{Q^2}\frac{d\ell_T^2}{\ell_T^2} \times \int_{z_h}^1 \frac{dz}{z}\left[\Delta\gamma_{q\to qg}(z,\ell_T^2)D_q^h(\frac{z_h}{z}) + \Delta\gamma_{q\to gq}(z,\ell_T^2)D_g^h(\frac{z_h}{z})\right], \quad (1)$$

which take a form very similar to the vacuum bremsstrahlung corrections that lead to the evolution equations in pQCD for fragmentation functions, except that the medium modified splitting functions, $\Delta\gamma_{q\to qg}(z,\ell_T^2)$ and $\Delta\gamma_{q\to gq}(z,\ell_T^2) = \Delta\gamma_{q\to qg}(1-z,\ell_T^2)$ depend on the properties of the medium via the jet transport parameter $\hat{q}$,

$$\hat{q} = \rho\int dq_T^2 \frac{d\sigma}{dq_T^2} q_T^2. \quad (2)$$

or the average squared transverse momentum broadening per unit length, which is also related to the gluon distribution density of the medium [66, 67]. The corresponding quark energy loss can be expressed as [55, 66, 68],

$$\frac{\Delta E}{E} = \frac{2N_c\alpha_s}{\pi}\int dy^- dz d\ell_T^2 \frac{1+z^2}{\ell_T^4}\left(1-\frac{1-z}{2}\right)\hat{q}(E,y)\sin^2\left[\frac{y^-\ell_T^2}{4Ez(1-z)}\right], \quad (3)$$

in terms of the jet transport parameter. Note that we include an extra factor of $1-(1-z)/2$ as compared to that used in Refs. [66, 71] due to corrections beyond the helicity amplitude approximation [68].

According to the definition of jet transport parameter, we can assume it to be proportional to local parton density in a QGP and hadron density in a hadronic gas. Therefore, in a dynamical evolving medium, one can express it in general as [49, 55, 66]

$$\hat{q}(\tau, r) = \left[\hat{q}_0 \frac{\rho_{QGP}(\tau, r)}{\rho_{QGP}(\tau_0, 0)}(1-f) + \hat{q}_h(\tau, r)f\right]\cdot\frac{p^\mu u_\mu}{p_0}, \quad (4)$$

where ρ_{QGP} is the parton (quarks and gluon) density in an ideal gas at a given temperature, $f(\tau, r)$ is the fraction of the hadronic phase at any given space and time, $\hat{q}_0$ denotes the jet transport parameter at the center of the bulk medium in the QGP phase at the initial time τ_0, p^μ is the four momentum of the jet and u^μ is the four flow velocity in the collision frame. We assume the hadronic phase of the medium is described as a hadron resonance gas, in which the jet transport parameter is approximated as,

$$\hat{q}_h = \frac{\hat{q}_N}{\rho_N}\left[\frac{2}{3}\sum_M \rho_M(T) + \sum_B \rho_B(T)\right], \quad (5)$$

where ρ_M and ρ_B are the meson and baryon density in the hadronic resonance gas at a given temperature, respectively, $\rho_N = n_0 \approx 0.17$ fm^{-3} is the nucleon density in the center of a large nucleus and the factor $2/3$ accounts for the ratio of constituent quark numbers in mesons and baryons. The jet transport parameter at the center of a large nucleus $\hat{q}_N$ has been studied in deeply inelastic scattering (DIS) [69, 70]. We use a recently extracted value [71] $\hat{q}_N \approx 0.02$ GeV^2/fm from the HERMES [72] experimental data. We will include all hadron resonances with mass below 1 GeV for the calculation of the hadron density at a given temperature T and zero chemical potential. We use a full 3+1D ideal hydrodynamics [73, 74] in our calculation to provide the space-time evolution of the local the local temperature and flow velocity in the bulk medium along the jet propagation path in heavy-ion collisions.

With the above medium modified fragmentation functions and temperature dependence of the jet transport coefficient, one can calculate the nuclear modification factor and compare to the experimental data as shown in Fig. 1. One obtains $\hat{q}_0\tau_0 = 0.54 - 0.63$ GeV^2 (with $\tau_0 = 0.6$) from the best fit to experimental data on pion spectra in the most 0-10% central $Au+Au$ collisions at $\sqrt{s} = 0.2$ TeV [55]. We assume that the jet transport coefficient is proportional to the initial parton density or the transverse density of charged hadron multiplicity in mid-rapidity. With the new ALICE data on charged particle pseudo-rapidity density at mid-rapidity $dN_{ch}/d\eta = 1584 \pm 4(stat.) \pm 76(sys.)$ [75]

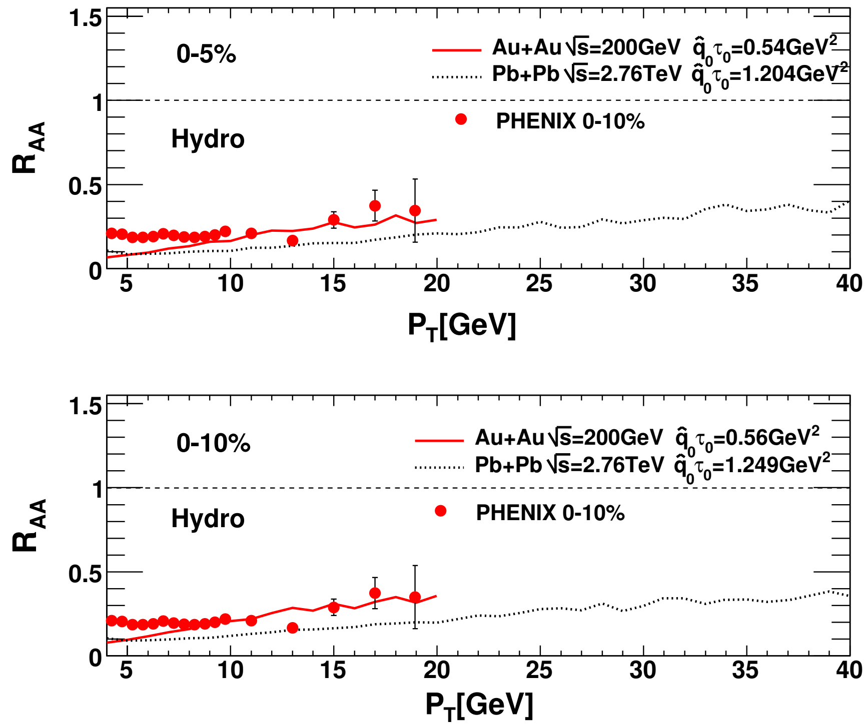

FIG. 1. Nuclear modification factor at mid-rapidity for neutral pion spectra in $0-5\%$ (upper panel) and $0-10\%$ (lower panel) central Au+Au collisions at $\sqrt{s} = 200$ GeV/n (solid lines) and $Pb+Pb$ collisions at $\sqrt{s} = 2.76$ TeV (dashed lines) as compared to PHENIX data [82] within the HT-BW model with $\hat{q}_0\tau_0 = 0.54$ GeV^2 and 1.2 GeV^2, respectively in the center of the most central collisions.

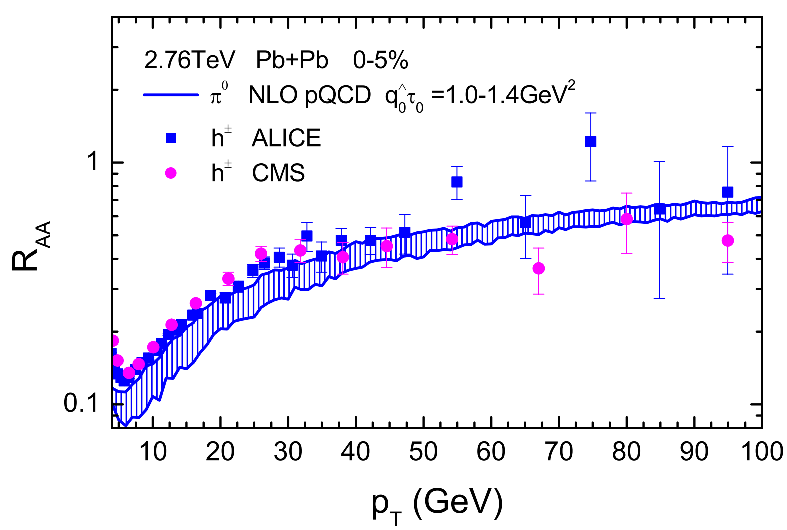

FIG. 2. The predicted nuclear modification factor [49] at mid-rapidity for neutral pion spectra in the most $0-5\%$ central $Pb+Pb$ collisions at $\sqrt{s} = 2.76$ TeV, within the HT-BW model with $\hat{q}_0\tau_0 = 1.0-1.4$ GeV^2 in the center of the most central collisions, as compared to data for charged hadrons from ALICE (filled square) [27] and CMS Experiment (filled circle) [26].

in the most central 5% $Pb+Pb$ collisions at $\sqrt{s}=2.76$ TeV versus $dN_{ch}/d\eta=687\pm 37$ for 0-5% Au+Au collisions at $\sqrt{s}=0.2$ TeV [76], we obtain the extrapolated value $\hat{q}_0\tau_0=1.0-1.4$ GeV^2 ($\tau_0=0.6$) for Pb+Pb collisions at $\sqrt{s}=2.76$ TeV. Shown in Fig. 7 (shaded curve) is the predicted nuclear modification factor for pion spectra in the 0-5% central Pb+Pb collisions at $\sqrt{s}=2.76$ TeV/n [49] as compared to the CMS [26] and ALICE [27] data. The best fit to the data gives us $\hat{q}_0\tau_0=0.9-1.2$ GeV^2.

IV. THE HIGHER-TWIST-MAJUMDER (HT-M) MODEL

The HT-M approach [48, 77] is a straightforward evaluation of the first power correction to the vacuum evolution of a fragmentation function. One calculates the medium modified fragmentation function by evolving an input fragmentation function using a vacuum plus medium modified kernel. As such, the formalism explicitly imbibes the concept of factorization [78]: the initial parton distribution functions are factorized from the hard scattering cross section, these are also factorized from the final fragmentation function. The cross section to produce hadrons at a given transverse momentum p_h and in a given rapidity interval y may be expressed as,

$$\frac{d\sigma}{dyd^2p_h}=\int d^2bd^2rT_{AB}(b,r)\int dx_adx_bG_A(x_a,Q^2)G_B(x_b,Q^2)\frac{d\hat{\sigma}}{d\hat{t}}\frac{\tilde{D}(z,Q^2)}{\pi z}. \quad (6)$$

In the equation above $T_{AB}(b,r)=\int dz\rho_A(z,\vec{r}+\vec{b}/2)\int dz'\rho_B(z',\vec{r}-\vec{b}/2)$, where $\rho_{A/B}$ represents the nuclear density in nucleus A/B. The nuclear parton distribution functions $G_A(x_A,Q^2)$ and $G_B(x_B,Q^2)$ are inclusive of any shadowing corrections. The modified fragmentation function $\tilde{D}$ contains two contributions: one from vacuum evolution which is contained in the regular DGLAP equations:

$$\frac{\partial D_q^h(z,Q^2)}{\partial\log(Q^2)}=\frac{\alpha_S(Q^2)}{2\pi}\int_z^1\frac{dy}{y}P_{q\to i}(y)D_i^h\left(\frac{z}{y},Q^2\right). \quad (7)$$

The second contribution to the modified fragmentation function is from the medium modified evolution equation [79],

$$\frac{\partial D_q^h(z,Q^2,q^-)|_{\zeta_i}^{\zeta_f}}{\partial\log(Q^2)}=\frac{\alpha_S}{2\pi}\int_z^1\frac{dy}{y}\int_{\zeta_i}^{\zeta_f}d\zeta P(y)K_{q^-,Q^2}(y,\zeta)D_q^h\left(\frac{z}{y},Q^2,q^-y\right)\Bigg|_{\zeta}^{\zeta_f}. \quad (8)$$

In both Eqs. (7) and (8), the splitting function $P_{q\to i}(y)$ is the regular Altarelli-Parisi splitting function. The modification from the medium is contained in the factor $K_{q^-,Q^2}(y,\zeta)$. All factors of the medium (such as the transport coefficients $\hat{q}$) are contained within this factor, along with phase factors that arise due to interference between different amplitudes of emission. The contribution to K from the leading power correction is given as,

$$K_{q^-,Q^2}(y,\zeta)=\frac{\left(\hat{q}(\zeta)-(1-y)\frac{\hat{q}}{2}+(1-y)^2\hat{q}_Q\right)}{Q^2}\left[2-2\cos\left(\frac{Q^2(\zeta-\zeta_i)}{2q^-y(1-y)}\right)\right]. \quad (9)$$

In the equation above, ζ and ζ_i represent the location of scattering and location of origin of the hard parton. The factor $\hat{q}(\zeta)$ without any subscripts represents the position (ζ) dependent transport coefficient of a gluon, which may be expressed in operator form as,

$$\hat{q}=\frac{8\pi^2\alpha_sC_A}{N_c^2-1}\int dy^-\langle X|Tr\left[F^{a\mu\nu}(y^-)v_\mu F_\nu^{a\sigma}v_\sigma\right]|X\rangle \quad (10)$$

where, $F^{a\mu\nu}$ is the position dependent field strength tensor of the gluon field and y^- represents the lightcone separation between these two field insertions. The state $|X\rangle$ represents the matter through which the jet propagates. Note that the $\hat{q}$ for a quark scattering off the gluon field is trivially related to the above expression as $\hat{q}_Q=\frac{C_F}{C_A}\hat{q}$.

In actual calculations of the nuclear modification factor, one assumes $\hat{q}$ to scale with some intrinsic quantity in the medium. In the calculations presented in this section, we will scale $\hat{q}$ with the entropy density s:

$$\hat{q}(s)=\hat{q}_0\frac{s}{s_0}. \quad (11)$$

In the equation above, s_0 is the maximum entropy density achieved in the center of the most central collision at top RHIC energy. The value of $\hat{q}=\hat{q}_0$ corresponds to this point. The space-time evolution of the entropy density is given by (2+1)D viscous hydrodynamic model [64, 65] tabulated by the hydro group within the JET Collaboration. One can now carry out parameter free calculations. The distance integral over K is then sampled over a large number of paths passing through the evolving medium. The starting points of all the paths are obtained by sampling the binary collision profile. The medium averaged length integral over K is then used to calculate the medium modified evolution of the fragmentation function using Eqs. (7) and (8).

Both medium and vacuum evolution equations require an input distribution. This is taken as a vacuum fragmentation function at the input scale of $Q_0 = p/L$, where $p = p_h/z$ it the transverse momentum of the parton which fragments to a hadron with transverse momentum p_h with a momentum fraction z. The factor L is the mean escape length of jets of that energy in the medium. The mean escape length is calculated by calculating the maximum length that could be travelled by a parton with an energy p using the single emission formalism of Guo and Wang [12, 13].

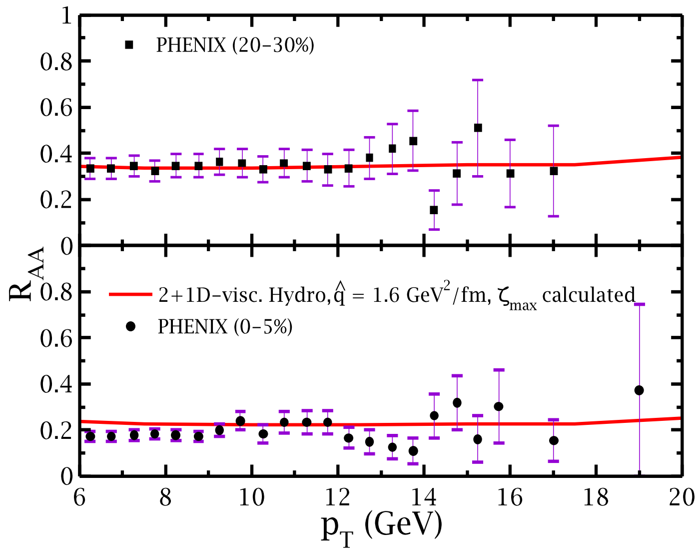

FIG. 3. The R_{AA} at two centralities at RHIC. The value around $p_h = 10$ GeV, in the $0-5\%$ centrality events, is used to find the value of $\hat{q}_0 = 1.6$ GeV^2/fm. The dependence of p_h and centrality are predictions.

In Fig. 3, we present calculations at two centralities in RHIC collisions. The lower panel represents $0-5\%$ collisions. The value of R_{AA} around a $p_h \sim 10$ GeV is used to set the value of $\hat{q}_0 = 1.6$ GeV^2/fm at the highest entropy density achieved at top RHIC energies. the dependence on p_h and centrality are predictions. In Fig. 4 we present calculations of the R_{AA} at central events at the LHC. The solid line represents a parameter free extrapolation to the LHC, i.e., the relation between $\hat{q}$ and the entropy density, as deduced at RHIC, is left unchanged. The upper dashed and lower dot-dashed line represents the result of decreasing and increasing the value of $\hat{q}$ by 20%.

The results presented here represent updates of calculations that have appeared in Ref. [50]. The fluid dynamical simulations have be been updated to include a new initial state and averaged over an ensemble of fluctuating initial conditions. Unlike previous calculations, the binary collision profile which determines the distribution of jet origins is also consistently determined by averaging over the same ensemble of initial conditions.

V. MARTINI-AMY MODEL

In the factorized picture, jet productions in relativistic heavy ion collisions proceed in stages. The first stage is the collision of initial state partons. Since the energy and the virtuality of these partons are $O(\sqrt{s})$, this stage takes place well before the formation of QGP. The second stage is the propagation of the scattered partons in the produced QGP. In the MARTINI-AMY approach of jet quenching [42, 80], the nuclear initial parton scatterings for jet production are carried out by using PYTHIA-8 on each nucleon-nucleon collisions with Glauber geometry. The propagation of jet partons is then carried out by solving the following rate equations using Monte-Carlo methods

$$\frac{dP_{q\bar{q}}(p)}{dt} = \int_k P_{q\bar{q}}(p+k)\frac{d\Gamma^q_{qg}(p+k,k)}{dk} - \int_k P_{q\bar{q}}(p)\frac{d\Gamma^q_{qg}(p,k)}{dk} + 2\int_k P_g(p+k)\frac{d\Gamma^g_{q\bar{q}}(p+k,k)}{dk} \,,$$

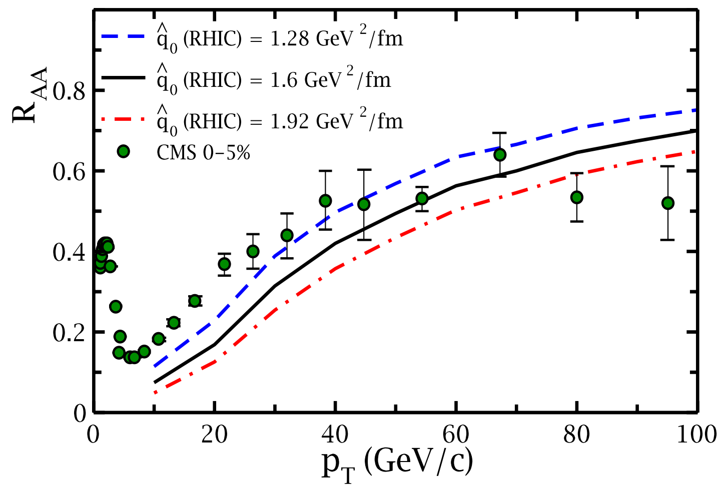

FIG. 4. The R_{AA} in $0-5\%$ central events at the LHC. The central solid line is a prediction based on the scaling of $\hat{q}$ with entropy density as obtained at RHIC. The upper dashed and lower dot-dashed lines represent a 20% downward and 20% upward shift in $\hat{q}$ respectively.

$$\frac{dP_g(p)}{dt} = \int_k P_{q\bar{q}}(p+k)\frac{d\Gamma^q_{qg}(p+k,p)}{dk} + \int_k P_g(p+k)\frac{d\Gamma^g_{gg}(p+k,k)}{dk} - \int_k P_g(p)\left(\frac{d\Gamma^g_{q\bar{q}}(p,k)}{dk} + \frac{d\Gamma^g_{gg}(p,k)}{dk}\Theta(k-p/2)\right) \quad (12)$$

where $d\Gamma^a_{bc}(p,k)/dk$ is the $a \to b+c$ splitting rate calculated in the full leading order thermal QCD that includes the HTL effects and the LPM effects. All split partons with energy above a threshold (currently set to 4 time the local temperature) are kept track of until the partons fragment outside of QGP. Elastic scatterings are included in a similar way.

In this approach, the properties of the local medium enters through the local temperature and the flow velocity when calculating the rates, and the interaction between the parton and the medium is controlled by the HTL resummed elastic collision rate

$$\frac{d\Gamma_{\rm el}}{d^2\mathbf{q}_\perp} = \frac{C_s}{(2\pi)^2}\frac{g_{\rm s}^2 m_D^2 T}{\mathbf{q}_\perp^2(\mathbf{q}_\perp^2 + m_D^2)} \quad (13)$$

where T is the fluid rest frame temperature, $g_{\rm s}$ is the coupling constant of the strong interaction and $m_D^2 = g_{\rm s}^2 T^2(2N_c + N_f)/6$ is the Debye mass squared. The factor C_s is the Casimir of the propagating parton. Hence, the average transverse momentum transfer squared per mean free path, $\hat{q} = \langle \mathbf{q}_\perp^2 \rangle / l_{\rm mfp}$, is not a primary parameter of the calculation but a derived quantity. In the fluid rest frame, it is given by

$$\hat{q} = \int^{q_{\rm max}} d^2\mathbf{q}_\perp\, \mathbf{q}_\perp^2 \frac{d\Gamma_{\rm el}}{d^2\mathbf{q}_\perp} \quad (14)$$

where $q_{\rm max}$ is the UV cut-off. In a static medium, it is given by

$$\hat{q} = C_s \alpha_{\rm s} m_D^2 T \ln(1 + q_{\rm max}^2/m_D^2) \quad (15)$$

where $q_{\rm max} \approx 6ET$.

For RHIC, the best fit to the data within MARTINI-AMY is achieved with $\alpha_{\rm s} = 0.29$. For LHC, the best fit is achieved with $\alpha_{\rm s} = 0.27$. With these values of strong coupling constant, one can calculate both the temperature and energy dependence of the jet transport coefficient according to Eq. (15).

VI. JET TRANSPORT PARAMETER

In order to compare medium properties extracted from phenomenological studies of jet quenching within different approaches to parton energy loss, we will focus on the value of jet transport parameter $\hat{q}$ either directly extracted or

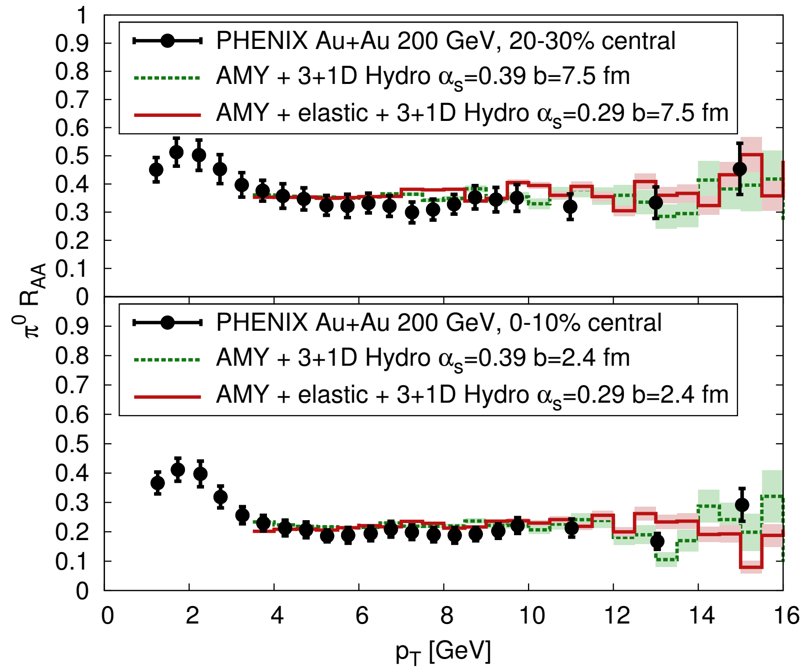

FIG. 5. The nuclear modification factors for the central Au-Au collisions at RHIC. The figure is from Ref.[81]. PHENIX data points are from [82]. The 3+1D ideal hydrodynamics calculation is from Ref.[83].

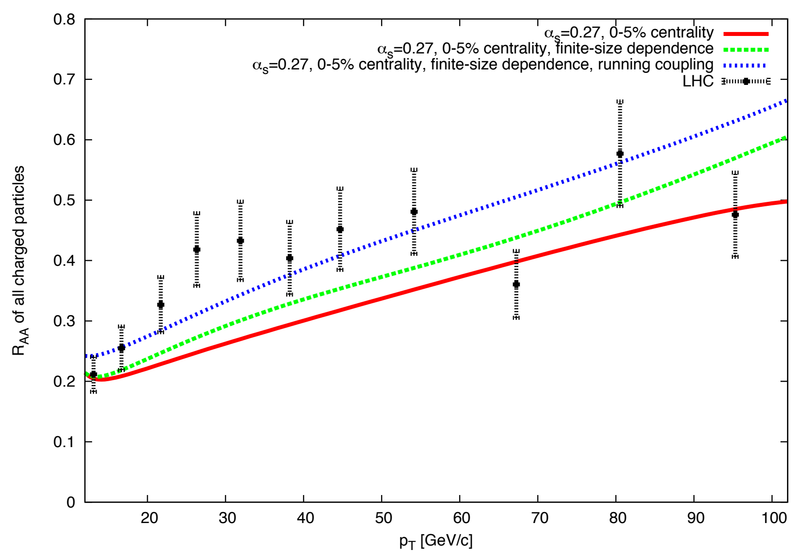

FIG. 6. The nuclear modification factors for the central Pb-Pb collisions at the LHC. The figure is from Ref.[84]. The 3+1D ideal hydrodynamics calculation is carried out using MUSIC [80].

evaluated within each model with the model parameters constrained by the experimental data. As a first step, we will only consider data on suppression factor of single inclusive hadron spectra $R_{AA}(p_T)$ at both RHIC and LHC. Within each model, $\hat{q}$ should be a function of both local temperature and jet energy which in turn varies along each jet propagation path. As a gauge of medium properties at its maximum density achieved in heavy-ion collisions, we will consider the value of $\hat{q}$ at the center of the most central A+A collisions at an initial time τ_0 when hydrodynamic models are applied for the bulk evolution. For all the hydrodynamic models used in this paper with different approaches of

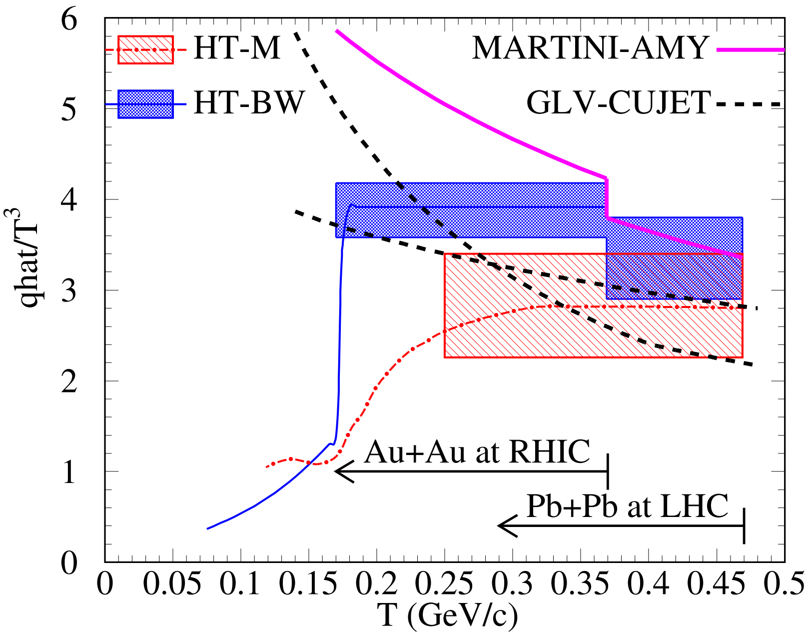

FIG. 7. The assumed temperature dependence of the scaled jet transport parameter $\hat{q}/T^3$ in different jet quenching models for an initial quark jet energy $E = 10$ GeV. Values of $\hat{q}$ at the center of the most central A+A collisions at an initial time $\tau_0 = 0.6$ fm/c in HT-BW and HT-M models are extracted from fitting to experimental data on hadron suppression factor R_{AA} at both RHIC and LHC. In GLV-CUJET and MARTINI-AMY model, it is calculated within the corresponding model with parameters as constrained by experimental data at RHIC and LHC. The arrows indicate the maximum temperatures reached at the center of the most central A+A collisions. See text for detailed explanations.

parton energy loss, the initial time is set at $\tau_0 = 0.6$ fm/c with initial temperature of $T_0 = 369$ and 469 MeV at the center of the most central Au+Au collisions at $\sqrt{s} = 200$ GeV at RHIC and Pb+Pb collisions at $\sqrt{s} = 2.76$ TeV at LHC, respectively.

Shown in Fig. 7 are extracted or calculated $\hat{q}$ as a function of the initial temperature for a quark jet with initial energy $E = 10$ GeV. For GLV-CUJET model, $\hat{q}$ calculated from two sets of parameters are shown, one with HTL screening mass and the maximum value of running coupling $\alpha_{\max} = 0.25$ and another with non-HTL screening mass which is twice that of HTL mass and $\alpha_{\max} = 0.4$. The values of $\hat{q}$ from MARTINI-AMY model are calculated according to the HTL formula in Eq. (15) with the two values of $\alpha_{\rm s}$ extracted from comparisons to the experimental data on R_{AA} at RHIC and LHC, respectively. Both GLV and MARTINI-AMY model assume zero parton energy loss and therefore zero $\hat{q}$ in hadronic phases. In HT-BW model, fit to experimental data gives gives $\hat{q} = 0.9 - 1.05$ GeV^2/fm at RHIC and 1.5 – 2 GeV^2/fm. Values of $\hat{q}$ in hadronic phases are calculated according to a hadron resonance gas model with the normalization in a cold nuclear matter determined by DIS data. Values of $\hat{q}$ in the QGP phase are considered proportional to T^3 and the coefficient is determined by fitting to the experimental data on R_{AA} at RHIC and LHC separately. In the HT-M model the procedure is similar except that $\hat{q}$ is assumed to be proportional to the local entropy density and its initial value in the center of the most central Au+Au collisions at RHIC is $\hat{q} = 0.57 - -0.85$ GeV^2/fm. In both HT approaches, no jet energy dependence of $\hat{q}$ is considered.

VII. CONCLUSIONS

We have carried out a survey study on the jet transport parameters extracted or calculated from four different approaches to the parton energy loss in dense medium whose parameters are constrained by the experimental data on suppression factors of large transverse momentum hadron spectra in high-energy heavy-ion collisions at both RHIC and LHC. We find that new data from LHC, combined with data from RHIC and advances in our understudying and modeling of jet quenching and bulk evolution, have provided unprecedented constraints on parton energy models. Our study here have significantly narrowed down the variation of $\hat{q}$ extracted from different model studies as compared to earlier efforts [53, 54]. The large range of p_T in experimental data and higher temperatures reached in the center of heavy-ion collisions also allowed a first investigation of the jet energy and temperature dependence of the jet transport coefficient. This is only a first step toward a systematic study of medium properties with hard probes constrained by experimental data on a wide variety of observables that should include dihadron and gamma-hadron correlations, single jets, dijets and gamma-jets suppressions, azimuthal asymmetries, modification of jet profile and jet fragmentation functions. All of these studies should be carried out within a realistic for jet quenching, hadronization and bulk evolution model that are also constrained by experimental data on bulk hadron spectra. With future precision and complimentary experiments at RHIC (sPHENIX) and LHC (ALICE, ATLAS and CMS) and theoretical advances in jet quenching and modeling of bulk evolution, one should be able to achieve a more quantitative understanding of the QGP properties in high-energy heavy-ion collisions.

ACKNOWLEDGEMENT

We would like to thank discussions with other members of the JET Collaboration. This work was supported by the Director, Office of Energy Research, Office of High Energy and Nuclear Physics, Division of Nuclear Physics, of the U.S. Department of Energy under Contract Nos. DE-AC02-05CH11231, DE-FG02-93ER40764, DE-AC02-98CH10886, DE-SC0004286 and within the framework of the JET Collaboration, by the NSF under grant number PHY-1207918, by the Natural Sciences and Engineering Research Council of Canada and by the National Natural Science Foundation of China under the grant No. 11221504.

[1] J. D. Bjorken, FERMILAB-PUB-82-059-THY, 1982.
[2] M. Gyulassy and M. Plumer, Phys. Lett. B **243**, 432 (1990).
[3] X. N. Wang and M. Gyulassy, Phys. Rev. Lett. **68**, 1480 (1992).
[4] M. Gyulassy and X. N. Wang, Nucl. Phys. B **420**, 583 (1994).
[5] R. Baier, Y. L. Dokshitzer, S. Peigne and D. Schiff, Phys. Lett. B **345**, 277 (1995).
[6] R. Baier, Y. L. Dokshitzer, A. H. Mueller, S. Peigne and D. Schiff, Nucl. Phys. B **484**, 265 (1997).
[7] B. G. Zakharov, JETP Lett. **63**, 952 (1996).
[8] M. Gyulassy, P. Levai and I. Vitev, Phys. Rev. Lett. **85**, 5535 (2000).
[9] M. Gyulassy, P. Levai and I. Vitev, Nucl. Phys. B **594**, 371 (2001).
[10] U. A. Wiedemann, Nucl. Phys. B **588**, 303 (2000).
[11] U. A. Wiedemann, Nucl. Phys. A **690**, 731 (2001).
[12] X. F. Guo and X. N. Wang, Phys. Rev. Lett. **85**, 3591 (2000).
[13] X. N. Wang and X. F. Guo, Nucl. Phys. A **696**, 788 (2001).
[14] P. Arnold, G. D. Moore and L. G. Yaffe, JHEP **0111**, 057 (2001).
[15] P. Arnold, G. D. Moore and L. G. Yaffe, JHEP **0206**, 030 (2002).
[16] X. N. Wang, Phys. Rev. C **61**, 064910 (2000).
[17] M. Gyulassy, I. Vitev and X. N. Wang, Phys. Rev. Lett. **86**, 2537 (2001).
[18] Proceedings of Hard Probes I, Int. J. Mod. Phys. **A10**, 2881-3090 (1995).
[19] Proceedings of Hard Probes Collaboration II, Int. J. Mod. Phys. **E12**, 147-271 (2002).
[20] J. Adams *et al.* [STAR Collaboration], Phys. Rev. Lett. **91**, 072304 (2003); Phys. Rev. Lett. **91**, 172302 (2003).
[21] S. S. Adler *et al.* [PHENIX Collaboration], Phys. Rev. Lett. **91**, 072301 (2003).
[22] C. Adler *et al.*, Phys. Rev. Lett. **90**, 082302 (2003).
[23] X. -N. Wang, Z. Huang, I. Sarcevic, Phys. Rev. Lett. **77**, 231-234 (1996). [hep-ph/9605213].
[24] A. Adare *et al.* [PHENIX Collaboration], Phys. Rev. C **80**, 024908 (2009) [arXiv:0903.3399 [nucl-ex]].
[25] B. I. Abelev *et al.* [STAR Collaboration], Phys. Rev. C **82**, 034909 (2010) [arXiv:0912.1871 [nucl-ex]].
[26] S. Chatrchyan *et al.* [CMS Collaboration], Eur. Phys. J. C **72**, 1945 (2012) [arXiv:1202.2554 [nucl-ex]].
[27] B. Abelev *et al.* [ALICE Collaboration], Phys. Lett. B **720**, 52 (2013) [arXiv:1208.2711 [hep-ex]].
[28] K. Aamodt *et al.* [ALICE Collaboration], Phys. Rev. Lett. **108**, 092301 (2012) [arXiv:1110.0121 [nucl-ex]].

[29] I. Vitev and B. -W. Zhang, Phys. Rev. Lett. **104**, 132001 (2010).
[30] G. Aad *et al.* [ATLAS Collaboration], Phys. Lett. B **719**, 220 (2013) [arXiv:1208.1967 [hep-ex]].
[31] G. Aad *et al.* [ATLAS Collaboration], arXiv:1306.6469 [hep-ex].
[32] G. Aad *et al.*, Phys. Rev. Lett. **105**, 252303 (2010).
[33] S. Chatrchyan *et al.* [CMS Collaboration], Phys. Lett. B **712** (2012) 176 [arXiv:1202.5022 [nucl-ex]].
[34] CMS Collaboration, Phys. Lett. B **718**, 773 (2012).
[35] ATLAS Collaboration, Report No. ATLAS-CONF-2012-121.
[36] X. -N. Wang, Nucl. Phys. **A750**, 98-120 (2005). [nucl-th/0405017].
[37] I. Vitev and M. Gyulassy, Phys. Rev. Lett. **89**, 252301 (2002).
[38] X. N. Wang, Phys. Lett. B **595**, 165 (2004) [arXiv:nucl-th/0305010].
[39] K. J. Eskola, H. Honkanen, C. A. Salgado and U. A. Wiedemann, Nucl. Phys. A **747**, 511 (2005).
[40] T. Renk, Phys. Rev. C **74**, 024903 (2006).
[41] H. Zhang, J. F. Owens, E. Wang and X. N. Wang, Phys. Rev. Lett. **98**, 212301 (2007);
[42] G. Y. Qin, J. Ruppert, C. Gale, S. Jeon, G. D. Moore and M. G. Mustafa, Phys. Rev. Lett. **100**, 072301 (2008) [arXiv:0710.0605 [hep-ph]].
[43] T. Renk, Phys. Rev. **C74**, 034906 (2006). [hep-ph/0607166].
[44] H. Zhang, J. F. Owens, E. Wang and X.-N. Wang, Phys. Rev. Lett. **103**, 032302 (2009). [arXiv:0902.4000 [nucl-th]].
[45] G. Y. Qin, J. Ruppert, C. Gale, S. Jeon and G. D. Moore, Phys. Rev. C **80**, 054909 (2009) [arXiv:0906.3280 [hep-ph]].
[46] M. Gyulassy, I. Vitev, X. -N. Wang *et al.*, In *Hwa, R.C. (ed.) et al.: Quark gluon plasma* 123-191. [nucl-th/0302077].
[47] A. Kovner, U. A. Wiedemann, In *Hwa, R.C. (ed.) et al.: Quark gluon plasma* 192-248. [hep-ph/0304151].
[48] A. Majumder and M. Van Leeuwen, Prog. Part. Nucl. Phys. A **66**, 41 (2011) [arXiv:1002.2206 [hep-ph]].
[49] X. -F. Chen, T. Hirano, E. Wang, X. -N. Wang and H. Zhang, Phys. Rev. C **84**, 034902 (2011) [arXiv:1102.5614 [nucl-th]].
[50] A. Majumder and C. Shen, Phys. Rev. Lett. **109**, 202301 (2012) [arXiv:1103.0809 [hep-ph]].
[51] K. C. Zapp, F. Krauss and U. A. Wiedemann, JHEP **1303**, 080 (2013) [arXiv:1212.1599 [hep-ph]].
[52] T. Renk, Phys. Rev. C **88**, 014905 (2013) [arXiv:1302.3710 [hep-ph]].
[53] S. A. Bass, C. Gale, A. Majumder, C. Nonaka, G. Y. Qin, T. Renk and J. Ruppert, Phys. Rev. C **79**, 024901 (2009).
[54] N. Armesto, M. Cacciari, T. Hirano, J. L. Nagle and C. A. Salgado, arXiv:0907.0667 [hep-ph].
[55] X. -F. Chen, C. Greiner, E. Wang, X.-N. Wang and Z. Xu Phys. Rev. **C81**, 064908 (2010). [arXiv:1002.1165 [nucl-th]].
[56] M. Gyulassy, P. Levai and I. Vitev, NPB **594**, 371 (2001); I. Vitev and M. Gyulassy, PRL**89**, 252301 (2002)
[57] M. Djordjevic and M. Gyulassy, NPA **733**, 265 (2004); PRL **94**, 112301 (2005.)
[58] S. Wicks, W. Horowitz, M. Djordjevic and M. Gyulassy, NPA **784**, 426 (2007)
[59] M. Djordjevic and U. W. Heinz, PRL 101, 022302 (2008).
[60] A. Buzzatti and M. Gyulassy, CUJET1.0, PRL**108**, 022301 (2012).
[61] W. A. Horowitz and M. Gyulassy, NPA **872**, 265 (2011)
[62] A. Buzzatti and M. Gyulassy, NPA904-905 **2013**, 779c (2013);
[63] A. Buzzatti, J. Xu, and M. Gyulassy, CUJET2.0 in preparation.
[64] H. Song and U. W. Heinz, Phys. Rev. C **77**, 064901 (2008) [arXiv:0712.3715 [nucl-th]].
[65] Z. Qiu and U. W. Heinz, Phys. Rev. C **84**, 024911 (2011) [arXiv:1104.0650 [nucl-th]].
[66] J. Casalderrey-Solana and X. N. Wang, Phys. Rev. C **77**, 024902 (2008).
[67] R. Baier, Y. L. Dokshitzer, A. H. Mueller, S. Peigne and D. Schiff, Nucl. Phys. B **484**, 265 (1997).
[68] B. W. Zhang and X. N. Wang, Nucl. Phys. A **720**, 429 (2003).
[69] E. Wang and X. N. Wang, Phys. Rev. Lett. **89**, 162301 (2002).
[70] A. Majumder, E. Wang and X. N. Wang, Phys. Rev. Lett. **99**, 152301 (2007).
[71] W. T. Deng and X. N. Wang, Phys. Rev. C **81**, 024902 (2010).
[72] A. Airapetian *et al.* [HERMES Collaboration], Nucl. Phys. B **780**, 1 (2007).
[73] T. Hirano, Phys. Rev. C **65**, 011901 (2002).
[74] T. Hirano and K. Tsuda, Phys. Rev. C **66**, 054905 (2002).
[75] K. Aamodt *et al.* [The ALICE Collaboration], arXiv:1011.3916 [nucl-ex].
[76] K. Adcox et al. (PHENIX), Phys. Rev. Lett. 86, 3500 (2001), arXiv:nucl-ex/0012008.
[77] A. Majumder, Phys. Rev. D **85**, 014023 (2012) [arXiv:0912.2987 [nucl-th]].
[78] J. C. Collins, D. E. Soper and G. F. Sterman, Nucl. Phys. B **261**, 104 (1985); J. w. Qiu and G. F. Sterman, Nucl. Phys. B **353**, 137 (1991).
[79] A. Majumder, arXiv:0901.4516 [nucl-th].
[80] B. Schenke, S. Jeon and C. Gale, Phys. Rev. C **82**, 014903 (2010) [arXiv:1004.1408 [hep-ph]].
[81] B. Schenke, C. Gale and S. Jeon, Phys. Rev. C **80**, 054913 (2009) [arXiv:0909.2037 [hep-ph]].
[82] A. Adare *et al.* [PHENIX Collaboration], Phys. Rev. Lett. **101**, 232301 (2008) [arXiv:0801.4020 [nucl-ex]].
[83] C. Nonaka and S. A. Bass, Phys. Rev. C **75**, 014902 (2007) [nucl-th/0607018].
[84] C. Young, B. Schenke, S. Jeon and C. Gale, arXiv:1209.5679 [nucl-th].
[85] B. Schenke, C. Gale and G. -Y. Qin, Phys. Rev. C **79**, 054908 (2009) [arXiv:0901.3498 [hep-ph]].